Competing C-4 and C-5-Acyl Stabilization of Uronic Acid Glycosyl Cations.

Elferink, H.; Remmerswaal, W.A.; Houthuijs, K.J.; Jansen, O.; Hansen, T.; Rijs, A.M.; ... ; Boltje, T.J.

Chemistry–A European Journal
Research Article
doi.org/10.1002/chem.202201724
Chemistry Europe
European Chemical Societies Publishing
www.chemeurj.org

Competing C-4 and C-5-Acyl Stabilization of Uronic Acid Glycosyl Cations

Hidde Elferink[+],[a] Wouter A. Remmerswaal[+],[b] Kas J. Houthuijs[+],[c] Oscar Jansen,[c] Thomas Hansen,[b, d] Anouk M. Rijs,[c, e] Giel Berden,[c] Jonathan Martens,[c] Jos Oomens,*[c] Jeroen D. C. Codée,*[b] and Thomas J. Boltje*[a]

Abstract: Uronic acids are carbohydrates carrying a terminal carboxylic acid and have a unique reactivity in stereoselective glycosylation reactions. Herein, the competing intramolecular stabilization of uronic acid cations by the C-5 carboxylic acid or the C-4 acetyl group was studied with infrared ion spectroscopy (IRIS). IRIS reveals that a mixture of bridged ions is formed, in which the mixture is driven towards the C-1,C-5 dioxolanium ion when the C-5,C-2-relationship is *cis*, and towards the formation of the C-1,C-4 dioxepanium ion when this relation is *trans*. Isomer-population analysis and interconversion barrier computations show that the two bridged structures are not in dynamic equilibrium and that their ratio parallels the density functional theory computed stability of the structures. These studies reveal how the intrinsic interplay of the different functional groups influences the formation of the different regioisomeric products.

Introduction

The study of reactive intermediates formed in a chemical glycosylation, is of major interest in carbohydrate chemistry to obtain insight into the stereoselective formation of glycosidic bonds. These intermediates are often highly reactive and may be extremely short-lived, challenging their characterization. Using low-temperature NMR spectroscopy, Crich and co-workers were the first to identify and characterize anomeric triflates to support their intermediacy during glycosylation reactions.[1] Ever since, a wide variety of glycosyl triflates and related species have been reported.[2] The well-known directing effect of C-2-*O*-acyl groups has been substantiated by the identification of C-1,C-2-dioxolanium ions by trapping this bridged cation,[3] NMR analysis of the intermediate under reaction conditions[4] and DFT computations.[5] Advances in NMR hardware and software have paved the way to characterize intermediates that are even less stable and present in only minute quantities in the reaction mixture, such as anomeric β-triflates,[6] dioxanium ions formed from non-vicinal acyl groups[7] as well as the formation of reactive imidinium ions.[8] Despite these efforts, some intermediates are too unstable to be detected in solution, while there is strong indirect evidence for their role in the reaction mechanism.[9] For example, oxocarbenium ions[10] and glycosyl cations stabilized by non-vicinal acyl groups, have often been invoked as product forming intermediates.[11] Oxocarbenium ion intermediates have been studied extensively with computational chemistry,[5] superacid chemistry,[12] infrared ion spectroscopy (IRIS)[13] and combinations thereof.[14] While the existence of glycosyl cations stabilized by non-vicinal ester is a heavily debated topic,[11,15] their formation and structure in the gas phase has recently been well established through multiple IRIS[16] and computational studies.[5,17] Through a combination of IRIS, DFT calculations and a systematic series of model glycosylations, we previously assessed the potential role of non-vicinal esters in glycosylation reactions to find that the formation and stability of ester stabilized ions was highly dependent on the configuration of donor glycosides and the position on which the participating acyl group was mounted.

[a] *Dr. H. Elferink,[+] Dr. T. J. Boltje*
Institute for Molecules and Materials
Synthetic Organic Chemistry
Radboud University Nijmegen
Heyendaalseweg 135, 6525 AJ Nijmegen (The Netherlands)
E-mail: thomas.boltje@ru.nl

[b] *W. A. Remmerswaal,[+] Dr. T. Hansen, Prof. Dr. J. D. C. Codée*
Leiden Institute of Chemistry
Leiden University
Einsteinweg 55, 2333 CC Leiden (The Netherlands)
E-mail: jcodee@chem.leidenuniv.nl

[c] *K. J. Houthuijs,[+] O. Jansen, Prof. Dr. A. M. Rijs, Dr. G. Berden, Dr. J. Martens, Prof. Dr. J. Oomens*
Institute for Molecules and Materials, FELIX Laboratory
Radboud University Nijmegen
Toernooiveld 7, 6525 ED Nijmegen (The Netherlands)
E-mail: jos.oomens@ru.nl

[d] *Dr. T. Hansen*
Departament de Química Inorgànica i Orgànica & IQTUB
Universitat de Barcelona
08028 Barcelona (Spain)

[e] *Prof. Dr. A. M. Rijs*
Division of BioAnalytical Chemistry
Department of Chemistry and Pharmaceutical Sciences
AIMMS Amsterdam Institute of Molecular and Life Sciences
Vrije Univeristeit Amsterdam
De Boelelaan 1085, 1081 HV Amsterdam (The Netherlands)

[+] *These authors contributed equally to this work*

Supporting information for this article is available on the WWW under https://doi.org/10.1002/chem.202201724

We found that in case of C-3-acyl-mannosyl donors the formation of a bridged dioxanium ion was most pronounced and was subsequently shown to exist under relevant glycosylation conditions using chemical exchange saturation transfer NMR.[7]

Another example of anchimeric assistance of non-vicinal esters can be found in uronic acids, monosaccharides that carry a C-5 carboxyl group. Uronic acids are an important class of carbohydrates that are key components in various biomolecules including the glycan chains of saponins, glycosaminoglycans, bacterial polysaccharides, pectins and alginates.[18] Therefore, they have been attractive targets for synthesis. We have shown that C-5-carboxylate esters, present in uronic acid donors, can intercept oxocarbenium ions to form C-1,C-5-dioxolanium ions.[13] In our previous study on the formation of oxocarbenium and dioxolanium ions from a 4-*O*-acetyl mannuronic acid donor and we observed the formation of a major C-1,C-5 dioxolanium ion species, alongside a minor C-1,C-4 dioxepanium ion species.[17] Both bridged ions can readily form from the $^3H_4$ oxocarbenium, which represents the most stable mannuronic acid oxocarbenium ion conformer, placing the C-3, C-4 and C-5 groups in *pseudo*-axial position, donating electron density towards the anomeric center.[19] To understand the stereoelectronic factors that determine the relative stability of the regioisomeric ions formed from C-4-acetyl uronic acid donors, we here report a study on a set of glycosyl cations, generated from uronic acid donors, differing in stereochemistry at the C-2 and C-4 position. We focused on the most common type of pyranosyl uronic acids, i.e. glucuronic acid (GlcA), galacturonic acid (GalA) and mannuronic acid (ManA), and also included taluronic acid (TalA), as it shares the axial orientation of the C-4 group with GalA and the orientation of the axial C-2 hydroxy group with ManA.[20] We studied the ions generated from these donors by combining IRIS with quantum-chemical computations. The glycosyl cations were generated by tandem-MS and characterized by IRIS. The IR-ion spectra have revealed that both the C-1,C-4 and C-1,C-5 bridged ions can be formed and that the preferred isomer critically depends on the configuration at C-2. GlcA and GalA donor led to the preferential formation of C-1,C-4 dioxepanium ions, while ManA and TalA donors mainly provided C-1,C-5 dioxolanium ions. The mixture of isobaric bridged ions could be disentangled by a population analysis to establish their relative ratio. Furthermore, the ratio of the isobaric bridged ions could be correlated to the relative stability of the ions, as revealed by conformational energy landscape (CEL) maps, created using DFT computations. These results demonstrate the impact of the relative stereochemistry on the preferred stabilization by acyl groups on uronic acid donors and may lead to the development of new stereoselective glycosyl donors.

Results and discussion

The set of donor glycosides, **1**—**4**, used in this study is depicted in Figure 1 (see SI for a detailed description of the synthesis of new compounds).[21] Because the generation of the GalA and TalA glycosyl cations from the parent thioglycosides by collision induced dissociation (CID) produced a complex fragmentation pattern, we generated the corresponding sulfoxide donors for these two pyranosides. These donors ionize more readily and prevent alternative fragmentation pathways that lead to loss of overall signal (see Supporting Figure S2). We have previously investigated the participation of non-vicinal esters in the glucose, galactose and mannose series, and have found that both the C-4-acetyl glucosyl and galactosyl donors provide C-1,C-4-dioxepanium ions upon ionization and CID. Contrary, ionization and CID on the C-4-acetyl mannose donor led to the formation of a ring opened C-4,C-5-dioxolanium ion.[17] The ions formed from the analogous C-4-acetyl talose donor **5** have not been reported yet. To relate the structure of the ions generated from the C-4-acetyl TalA donor **4** to the structure of the ions lacking the C-5 carboxylic acid ester, we here generated donor **5** and studied the glycosyl cations derived from this precursor.

IR ion spectroscopy of uronic acid cations

The cations generated from **1**—**5** were characterized with IR ion spectroscopy using the FELIX infrared free electron laser

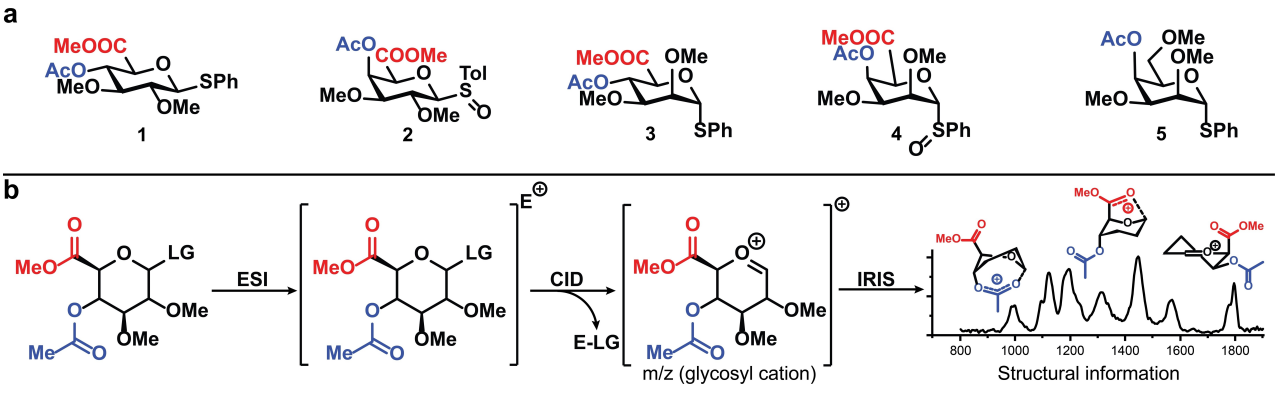

Figure 1. a) Ion precursors (**1**–**5**) used for IRIS-experiments. b) General overview of the workflow to generate and characterize glycosyl cations by IR-ion spectroscopy (IRIS). PG = protection group, LG = leaving group, and E = ammonium or proton.

operating between 750 and 1900 cm^{-1}.[22] This frequency range is well suited to distinguish between potential cation isomers: the glycosyl oxocarbenium ion, the C-1,C-4-dioxepanium ion and the C-1,C-5-dioxolanium ion. A significant difference in the O-C^+-O stretch is found between the C-1,C-4-dioxepanium ion (~1550 cm^{-1}) and the C-1,C-5-dioxolanium ion (~1650 cm^{-1}), which results from the difference in the vibration of the endocyclic vs. exocyclic OR group. Density-functional theory (DFT) and wave-function theory (WFT) computations were used to aid in the spectral assignment. Geometries and vibrational spectra of the cations were computed at the MP2/6-311++G(2d,2p)//B3LYP/6-31++G(d,p) level, which was found to model the vibrational frequencies well.[13,23] The measured IR-ion spectra of the GlcA cation **6** and GalA cation **7** are shown in Figure 2a-d (black line) and they contain several diagnostic peaks. In contrast to the IR ion spectrum of the ManA cation **8** (depicted in Figure 2e—f), a high intensity band at 1550 cm^{-1} is observed, corresponding to the O-C^+-O stretch of an endocyclic C-1,C-4-dioxepanium ion. Comparison with the calculated spectra of the C-1,C-4 dioxepanium (filled blue spectra) and C-1,C-5 dioxolanium (filled red spectra) ion shows good overlap for the former ion. Of note, minor bands (most notably at 1650 cm^{-1}) are observed in the spectra of the GluA and GalA ions, which suggest a mixture of species in which the C-1,C-5 dioxolanium ion is present as a minor fraction. Indeed, an improved spectral match is obtained from a weighted average of the computational spectra of the C-1,C-4 dioxepanium and C-1,C-5 dioxolanium ions (see Supporting Figure S6). The optimum mixing ratio is determined by minimizing the root-mean-square deviation between the experimental spectrum and the averaged computed spectra,[24] giving 9% and 20% contributions of the C-1,C-5 dioxolanium ion to the total population for GluA and GalA, respectively. In both cases, the calculated spectra of the oxocarbenium and previously observed ring-opened ions show poor overlap with the measured spectra (see Supporting Figure S7).

As was reported previously, the ManA donor ionizes to preferentially provide the C-1,C-5-dioxolanium ion, with the C-1,C-4-dioxepanium ion being present in minor amounts (Figure 2e). For the TalA cation **10**, a strong absorption is observed at 1650 cm^{-1} (Figure 3c and 3d), indicative of the C-1,C-5-dioxolanium ion. The C-1,C-4-dioxepanium ion stretch vibration is also apparent in the spectrum at 1550 cm^{-1}, suggesting the presence of this ion as a minor species. To benchmark the stabilization of the TalA ion, talose donor **5** was ionized, yielding, after CID, the IRIS spectrum shown in Figure 3a,b. The

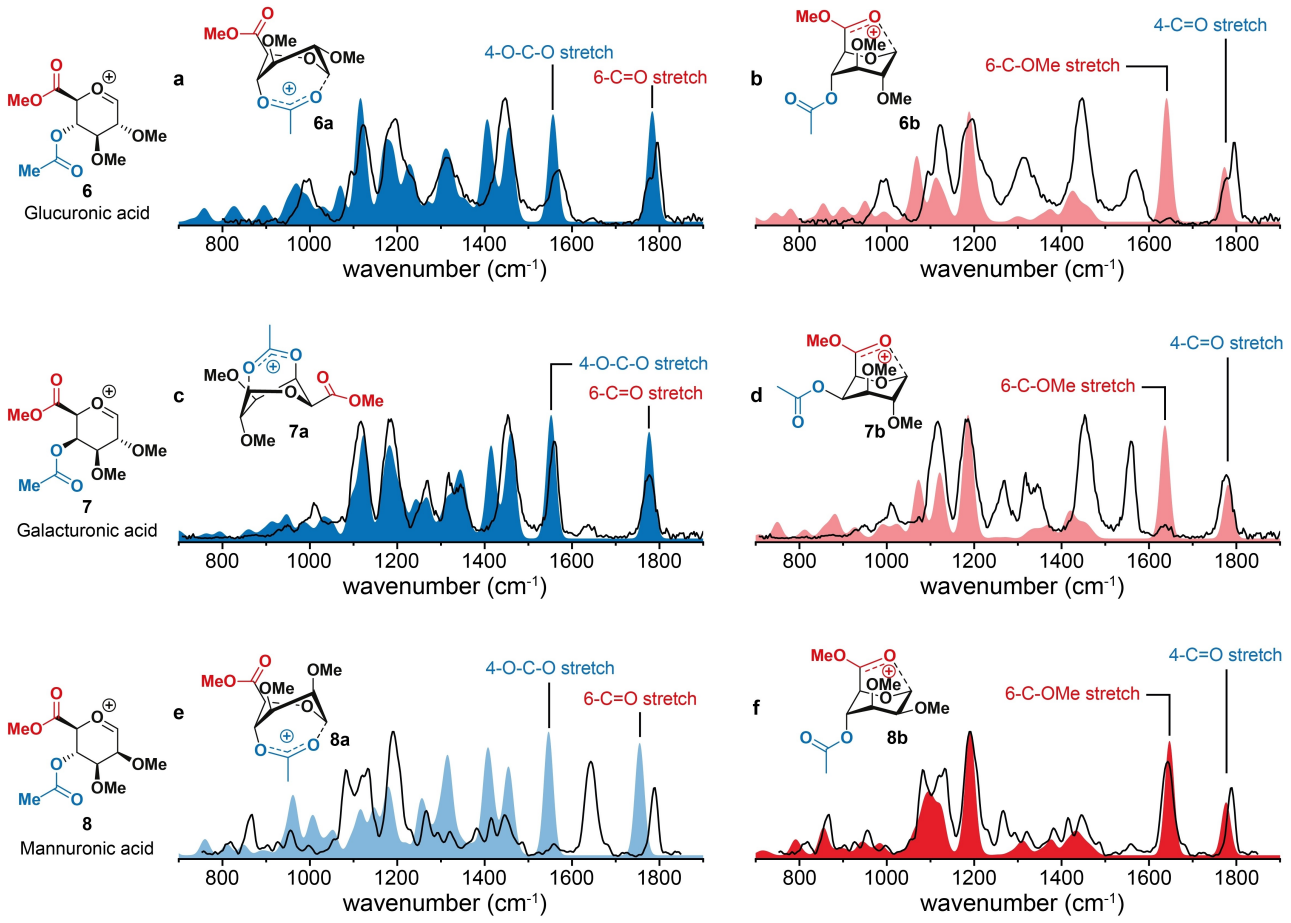

Figure 2. IR ion spectra of uronic acid cations **6**, **7** and **8**. Comparison of the measured IR-ion spectrum (black line) of **6**, **7** and **8** with the calculated spectra (filled) of C-4 (a, c and e in blue) or C-5 (b, d and f in red) stabilization. The assigned major and minor isomers are represented by the full-color and opaque-color spectra, respectively. Panel e and f are adapted from Elferink et al.[13]

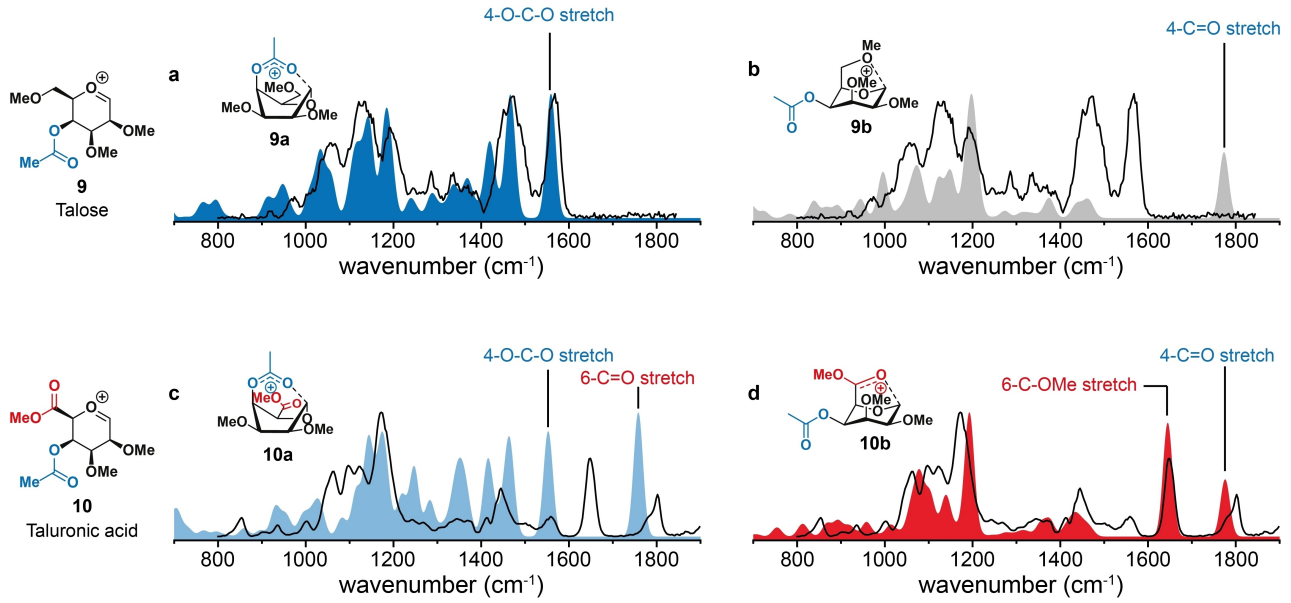

Figure 3. IR ion spectra of talosyl cations **9** and **10**. Comparison of the measured IR-ion spectrum (black line) of **9** and **10** with the calculated spectra (filled) of C-4 (a and c in red) or C-5 (b in gray and d in red) stabilization. The assigned major and minor isomers are represented by the full-color and opaque-color spectra, respectively.

calculated spectrum of the talosyl oxocarbenium gave poor overlap with the recorded spectrum, while the C-1,C-4-dioxepanium ion matched well. This indicates that formation of the C-1,C-4-dioxepanium ion by the attack of the axial C-4 acetyl group on the anomeric oxocarbenium ion can take place to provide a more stable ion. Thus, while the talosyl ion resembles the galactosyl ion in terms of dioxepanium ion formation and not the mannosyl ion, the TalA ion more closely matches the ManA system and provides the C-1,C-5 dioxolanium ion as the major species. Again, the contribution of the minor species can be estimated by optimizing the weighted average of the computed spectra, which gives contributions of 23% and 34% of the C-1,C-4 dioxepanium ion to the total population for ManA and TalA, respectively (see Supporting Figure S6).

CEL maps of glycosyl cations

In order to understand the preference for the formation of C-1,C-4 or C-1,C-5 bridged ions, we computationally investigated the stability of these ions. Recently, we have assessed the relative stability of glycosyl cations, in which ester participation and oxocarbenium ion formation were in competition, using a DFT protocol to compute the conformational energy landscape (CEL) for these ions.[14,25] This method maps the energy of glycosyl cations as a function of their shape by probing the complete conformational space that these cations can occupy, see Figure 4a.[26] Here, we took four key rotamers into account, differing in (1) the orientation of the C-4 acetate group, pointing either towards the anomeric C-1 (rotamer 1; R1) or away from C-1 (rotamer 2, R2), and (2) the orientation of the C-5 uronic acid moiety, pointing either towards C-1 in an eclipsed conformation (ecl) or away from C-1 in a bisected conformation (bis). This yields four rotamers, i.e. R1-ecl, R1-bis, R2-ecl and R2-bis (Figure 4b). The CEL maps were computed in the gas phase using MP2/6-311++G(2d,2p)//B3LYP/6-311G(d,p), this method was shown to provide accurate energies which correlate well with experimental results[14] (for more information see the Supporting Information). Figure 4 depicts the CEL maps of the four uronic acids: GlcA (Figure 4c), GalA (Figure 4d), ManA (Figure 4e) and TalA (Figure 4f), in which the R1-ecl is shown on the left side and R2-ecl rotamers on the right side. The bisected C-5 carboxylate rotamers for the glycosyl cations were computed to be significantly higher in energy for all isomers and are therefore not depicted (see Supporting Figure S18 and S9 for all CEL maps).

The CEL maps show that GlcA and GalA have a strong preference for the formation of a C-1,C-4 dioxepanium ion ($\Delta\Delta G^\circ = 2.1$ and 4.8 kcal mol^{-1}, respectively) over other cations, with the GlcA C-1,C-4 dioxepanium ion preferentially taking up a $^5S_1$-like conformation and the GalA C-1,C-4-dioxepanium ion in a $^1S_5$-like skew boat form. In contrast, for ManA and TalA, the CEL maps show that the C-1,C-5 dioxolanium ions in a $^1C_4$-like conformation are more favorable ($\Delta\Delta G^\circ = 3.2$ and 0.3 kcal mol^{-1}). The maps reveal that the TalA C-1,C-4 and C-1,C-5 bridged ions are very close in energy. From the lowest energy structures, it can be deduced that the orientation of the C-2-substituent plays an important role in shaping the stability of the C-1,C-5-dioxiolanium ions. In the ManA and TalA ions, the C-2-Ome group takes up a sterically favorable *pseudo*-equatorial position. Hyperconjugative stabilization by donation of electron density of the axial σ_{C2-H2} bond in the $\sigma^*_{C1\text{-}O+}$ (a stabilizing gauche effect) may also contribute favorably.[27] The GlcA and

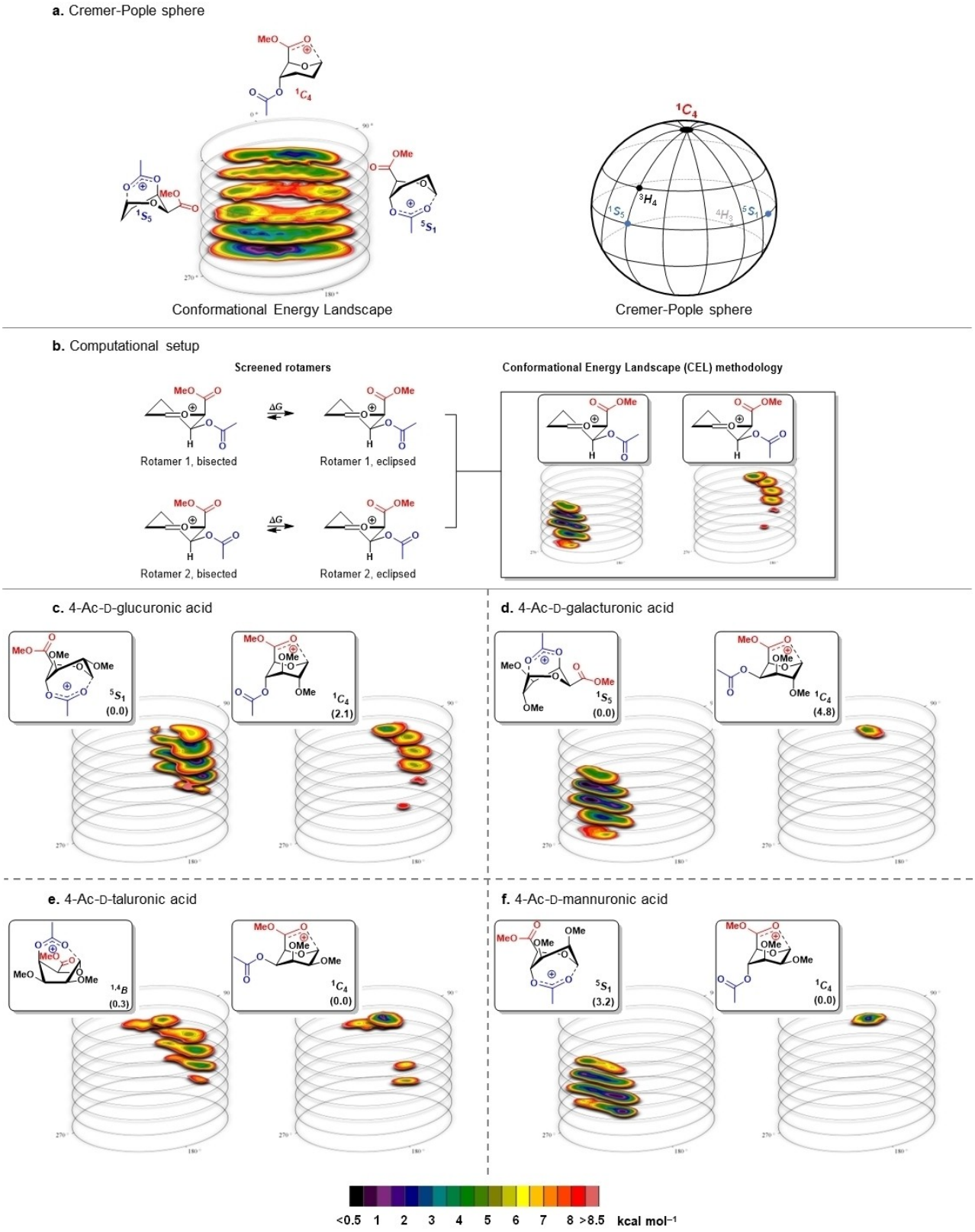

Figure 4. CEL maps of 2,3-*O*-Me-4-*O*-Ac-D-uronic acid cations in which the local minima identified are shown with their respective energy. a. The Cremer-Pople sphere. b. The used computational protocol. Two acetyl ester (R1 and R2) and two methoxy-acid rotamers (eclipsed and bisected) were considered for all computed glycosyl cations generating four CEL maps (R1 bisected, R1 eclipsed, R2 bisected, R2 eclipsed). Only eclipsing methoxy-acid rotamers are shown since they are lower in energy than the corresponding bisecting rotamers. All energies are as computed at MP2/6-311++G(2d,2p)//B3LYP/6-311G(d,p) at 298.15 K and expressed as gas phase Gibbs free energy in kcal mol^{-1}. CEL maps for (c) glucuronic acid, (d) galacturonic acid, (e) taluronic acid, and (f) mannuronic acid cations.

GalA C-1,C-5-dioxolanium ions on the other hand place their C-2-substituents in an unfavorable axial position. In the TalA and ManA C-1,C-4-dioxepanium ions, the C-2- and C-3-groups experience destabilizing eclipsing interactions, which are absent in the GlcA and GalA C-1,C-4-dioxepanium ions. The lowest energy structures of the GlcA and ManA C-1,C-4- and C-1,C-5-dioxolanium ions can be found in the same region of the CEL map, because the relative orientation of the C-4 and C-5 substituents is *trans*. In contrast, the C-1,C-4- and C-1,C-5 bridged ions in the GalA and TalA case, having *cis* C-4 and C-5 groups, are found in opposite regions of the conformational space. This indicates that greater conformational changes are required for the interconversions between the two conformations for GalA and TalA than for GlcA and ManA, likely requiring a higher interconversion barrier. We confirmed this by computing the reaction profile of this interconversion (see Supporting Table S1 and Supporting Figures S10–13 for the complete reaction profiles), showing higher barriers for GalA and TalA ($\Delta G^{\ddagger} = 18.4$ and 23.5 kcal mol^{-1}, respectively) than for GlcA and ManA ($\Delta G^{\ddagger} = 14.3$ and 13.8 kcal mol^{-1}, respectively).

Isomer population analysis

To experimentally determine the relative population of the different cationic species, we performed an isomer population analysis (Figure 5). In this experiment, the irradiation occurs at specific IR frequencies, which are diagnostic for one of the isomers. The ion population is irradiated with an increasing number of laser pulses to fragment the absorbing ions.[28] The normalized precursor depletion ($[1-I_{precursor}/I_{total}]\times 100\,\%$) is plotted as a function of the number of laser pulses to generate an ion depletion curve. When depletion curves do not converge to 100 %, this indicates the presence of isomeric structures, which do not absorb at the selected IR wavelength and whose relative abundance can thus be determined. First, we studied the stability of the isolated glycosyl cations by varying the isolation time. In the case of galacturonic acid **7** and taluronic acid **10**, no significant time-dependent auto-fragmentation was observed. In contrast, mannuronic acid **8** and glucuronic acid cation **6** showed auto-fragmentation over time, and thus could not be used for isomer population analysis.

The isomer population analysis on the GalA and TalA ions **7** and **10** was performed at approximately 1565 cm^{-1} and approximately 1635 cm^{-1} (diagnostic for C-4 participation and C-5 participation, respectively). As a control experiment, measurements were performed at a frequency where both isomers are predicted to absorb (ca. 1200 cm^{-1}). The control experiments show complete depletion of the parent ion mass, confirming a common frequency region of absorption. Next, we explored the depletion of the C-1,C-4 dioxepanium ion diagnostic peak at ~1565 cm^{-1}. In the case of galacturonic acid **7**, a sharp decrease in ion population was observed, resulting in ~90 % depletion, as determined by the fitted exponential decay (grey line). In line with the computational results, this reveals the C-1,C-4 dioxepanium ion isomer as the major species in the mixture of galacturonic acid cations. In contrast, the ion population of taluronic acid at 1563 cm^{-1} showed a plateau at ~30 % depletion, indicating that the TalA C-1,C-4-dioxepanium ion is not the major species in the ion mixture. Subsequently, we measured the ion populations at ~1635 cm^{-1} (diagnostic for C-5 stabilization). For galacturonic acid **7** a plateau was reached at around 10 %, which agrees well with the presence of the C-1,C-4-dioxepanium ion in the mixture being approximately 90 %. In the case of the TalA ion **10**, a ~65 % depletion of the ion population was observed, indicating the C-1,C-5 dioxolanium ion to be the major species in the gas-phase ion mixture, which corresponds well with the presence of the C-1,C-4-dioxepanium ion at about 30 % in the mixture, as derived from irradiation at 1563 cm^{-1}. The relative ratio of isomers roughly

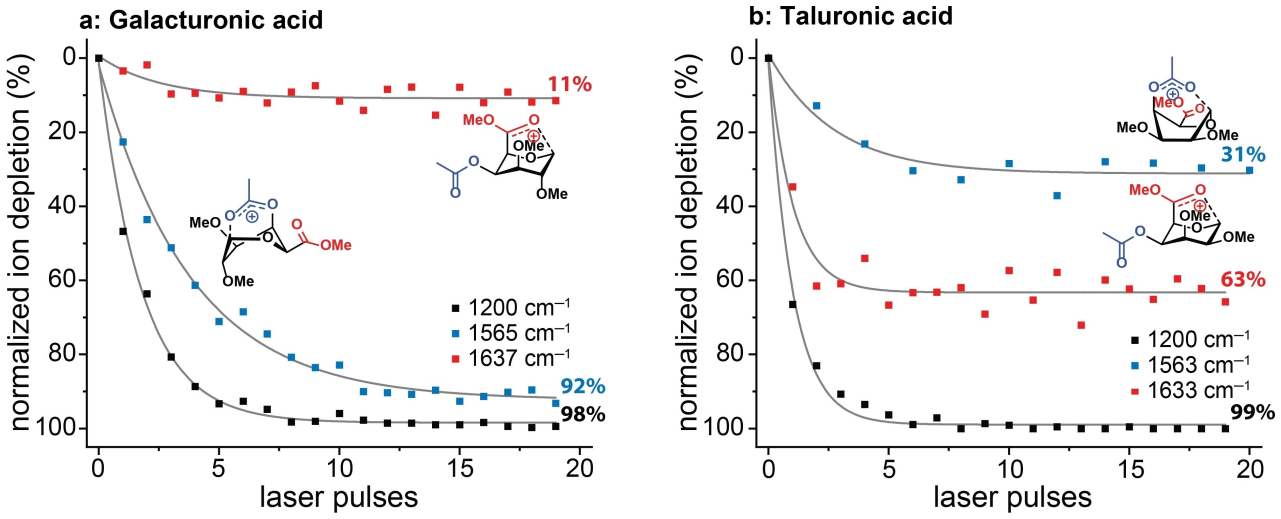

Figure 5. Isomer population analysis of cations **7** and **10**. The laser was set on frequencies characteristic for C-4 participation (blue squares), the C-5 participation (red squares). As control a frequency was used, in which both structures are predicted to absorb (black squares). The experimental data were fitted with a single exponential decay (grey lines). a) Isomer population analysis of cation **7**. b) Isomer population analysis of cation **10**.

corresponds to the stability of the ions as established with the CEL computations. The population analyses demonstrate that the contribution of the minor species (11% and 31%) is lower than was estimated by mixing of the computational spectra by minimization of the RMS deviation from experiment (20% and 34%). The contribution of very minor species might be overestimated by this method as it broadens the mixed computed spectrum, reducing spectral mismatch caused by slight frequency shifts.

Of note, the fact that we can selectively deplete the mixture of either component, indicates that under the experimental conditions the C-1,C-4- and C-1,C-5-bridged ions do not equilibrate on the experimental time-scale of 2 seconds (20 laser pulses at 10 Hz). Indeed, the computed reaction profile for the interconversion of both isomers (see Supporting Table S1 and Supporting Figures S10-13), shows a significant barrier (18.4 and 23.5 kcal mol^{-1} for the GalA and TalA, respectively).

Conclusion

Through a combination of IR ion spectroscopy and quantum-chemical computations, the formation of uronic acid cations carrying a C-4-acyl group was studied to unravel the stabilization of uronic acid oxocarbenium ions by either the C-5 carboxylate or C-4-ester. A relationship between the formation of either a C-1,C-5 or C-1,C-4 bridged ion and the relative configuration of C-2 and C-5 was discovered. The competitive formation of the C-1,C-5 or C-1,C-4 bridged ions is driven towards the C-1,C-5 dioxolanium ion when the C-5,C-2-relationship is *cis*, as present in the mannuronic and taluronic acid, and towards the formation of the C-1,C-4 dioxepanium ion when this relation is *trans*, as in glucuronic and galacturonic acid. The distribution of the formed dioxolenium ions depends on the stability of both isomeric ions, and they are not in equilibrium under the experimental conditions of the IRIS experiments as determined by our isomer population analysis and in line with DFT computations. The CEL maps revealed structural features that play a role in determining the stability of the different glycosyl cations. Insight into the structure of glycosyl cations is of relevance to understand the reactivity and stereoselectivity of glycosyl donors in the assembly of oligosaccharides and glycoconjugates. Even though the ions under study here were generated in the gas phase, and the results of the study can therefore not directly be translated to a role in glycosylation reactions in solution, the study has revealed how the intrinsic interplay between different functional groups in these ions shapes their overall conformation and stability. The fact that C-1,C-4- and C-1,C-5 bridged ions can be formed and observed might be exploited in glycosylation reactions in which the reactivity and stereoselectivity of uronic acid donor glycosides can be controlled by the installation of (even more powerful participating) acyl-type functionalities.[28c,29]

Experimental section

See the Supporting Information for experimental and computational procedures and analytical data.

Acknowledgements

This work was supported by the Nederlandse Organisatie voor Wetenschappelijk Onderzoek (NWO-VICI grant VI.C.182.020 to JDCC, NWO-VIDI grant VI.Vidi.192.070 awarded to TJB and the research program "National Roadmap Grootschalige Wetenschappelijke Infastructuur" 184.034.022 awarded to HFML-FELIX) and SURFsara for computational resources [NWO Rekentijd Grant 2021.055 awarded to JO, NWO Rekentijd Grant 2021/ENW/01070753 awarded to JDCC].

Conflict of Interest

The authors declare no conflict of interest.

Data Availability Statement

The data that support the findings of this study are available in the supplementary material of this article.

Keywords: carbohydrates · computational chemistry · IR spectroscopy · reaction mechanisms

[1] D. Crich, S. Sun, *J. Am. Chem. Soc.* **1997**, *119*, 11217–11223.
[2] T. G. Frihed, M. Bols, C. M. Pedersen, *Chem. Rev.* **2015**, *115*, 4963–5013.
[3] C. U. Pittman, S. P. McManus, J. W. Larsen, *Chem. Rev.* **1972**, *72*, 357–438.
[4] D. Crich, Z. Dai, S. Gastaldi, *J. Org. Chem.* **1999**, *64*, 5224–5229.
[5] T. Nukada, A. Berces, M. Z. Zgierski, D. M. Whitfield, *J. Am. Chem. Soc.* **1998**, *120*, 13291–13295.
[6] A. G. Santana, L. Montalvillo-Jiménez, L. Díaz-Casado, F. Corzana, P. Merino, F. J. Cañada, G. Jiménez-Osés, J. Jiménez-Barbero, A. M. Gómez, J. L. Asensio, *J. Am. Chem. Soc.* **2020**, *142*, 12501–12514.
[7] F. F. J. de Kleijne, H. Elferink, S. J. Moons, P. B. White, T. J. Boltje, *Angew. Chem. Int. Ed.* **2022**, *61*, e202109874.
[8] a) Y. Qiao, W. Ge, L. Jia, X. Hou, Y. Wang, C. M. Pedersen, *Chem. Commun.* **2016**, *52*, 11418–11421; b) S.-R. Lu, Y.-H. Lai, J.-H. Chen, C.-Y. Liu, K.-K. T. Mong, *Angew. Chem. Int. Ed.* **2011**, *50*, 7315–7320; *Angew. Chem.* **2011**, *123*, 7453–7458.
[9] a) J. I. Seeman, *Chem. Rev.* **1983**, *83*, 83–134; b) J. I. Seeman, *J. Chem. Educ.* **1986**, *63*, 42.
[10] a) A. Franconetti, A. Ardá, J. L. Asensio, Y. Blériot, S. Thibaudeau, J. Jiménez-Barbero, *Acc. Chem. Res.* **2021**, *54*, 2552–2564; b) P. Merino, I. Delso, S. Pereira, S. Orta, M. Pedrón, T. Tejero, *Org. Biomol. Chem.* **2021**, *19*, 2350–2365.
[11] A. A. Hettikankanamalage, R. Lassfolk, F. S. Ekholm, R. Leino, D. Crich, *Chem. Rev.* **2020**, *120*, 7104–7151.
[12] a) A. Martin, A. Arda, J. Désiré, A. Martin-Mingot, N. Probst, P. Sinaÿ, J. Jiménez-Barbero, S. Thibaudeau, Y. Blériot, *Nat. Chem.* **2016**, *8*, 186–191; b) L. Lebedel, A. Ardá, A. Martin, J. Désiré, A. Mingot, M. Aufiero, N. Aiguabella Font, R. Gilmour, J. Jiménez-Barbero, Y. Blériot, S. Thibaudeau, *Angew. Chem. Int. Ed.* **2019**, *58*, 13758–13762; *Angew. Chem.* **2019**, *131*, 13896–13900.
[13] a) H. Elferink, M. E. Severijnen, J. Martens, R. A. Mensink, G. Berden, J. Oomens, F. P. J. T. Rutjes, A. M. Rijs, T. J. Boltje, *J. Am. Chem. Soc.* **2018**, *140*, 6034–6038; b) F. ter Braak, H. Elferink, K. J. Houthuijs, J. Oomens, J. Martens, T. J. Boltje, *Acc. Chem. Res.* **2022**, *55*, 1669–1679.

[14] T. Hansen, L. Lebedel, W. A. Remmerswaal, S. van der Vorm, D. P. A. Wander, M. Somers, H. S. Overkleeft, D. V. Filippov, J. Désiré, A. Mingot, Y. Bleriot, G. A. van der Marel, S. Thibaudeau, J. D. C. Codée, *ACS Cent. Sci.* **2019**, *5*, 781–788.
[15] a) K. Upadhyaya, Y. P. Subedi, D. Crich, *Angew. Chem. Int. Ed.* **2021**, *60*, 25397–25403; b) D. Crich, *J. Am. Chem. Soc.* **2021**, *143*, 17–34.
[16] a) E. Mucha, M. Marianski, F.-F. Xu, D. A. Thomas, G. Meijer, G. von Helden, P. H. Seeberger, K. Pagel, *Nat. Commun.* **2018**, *9*, 4174; b) M. Marianski, E. Mucha, K. Greis, S. Moon, A. Pardo, C. Kirschbaum, D. A. Thomas, G. Meijer, G. von Helden, K. Gilmore, P. H. Seeberger, K. Pagel, *Angew. Chem. Int. Ed.* **2020**, *59*, 6166–6171; *Angew. Chem.* **2020**, *132*, 6224–6229; c) K. Greis, C. Kirschbaum, G. Fittolani, E. Mucha, R. Chang, G. von Helden, G. Meijer, M. Delbianco, P. H. Seeberger, K. Pagel, *Eur. J. Org. Chem.* **2022**, *2022*, e202200255; d) H. Elferink, R. A. Mensink, W. W. A. Castelijns, O. Jansen, J. P. J. Bruekers, J. Martens, J. Oomens, A. M. Rijs, T. J. Boltje, *Angew. Chem. Int. Ed.* **2019**, *58*, 8746–8751; *Angew. Chem.* **2019**, *131*, 8838–8843.
[17] a) A. Bérces, G. Enright, T. Nukada, D. M. Whitfield, *J. Am. Chem. Soc.* **2001**, *123*, 5460–5464; b) T. Nukada, A. Bérces, D. M. Whitfield, *Carbohydr. Res.* **2002**, *337*, 765–774; c) D. M. Whitfield, T. Nukada, *Carbohydr. Res.* **2007**, *342*, 1291–1304; d) M. V. Panova, M. G. Medvedev, A. V. Orlova, L. O. Kononov, *ChemPhysChem* **2022**, *23*, e202100788; e) X. Liu, Y. Song, A. Liu, Y. Zhou, Q. Zhu, Y. Lin, H. Sun, K. Zhu, W. Liu, N. Ding, W. Xie, H. Sun, B. Yu, P. Xu, W. Li, *Angew. Chem. Int. Ed.* **2022**, *61*, e20220151; f) T. Hansen, H. Elferink, J. M. A. van Hengst, K. J. Houthuijs, W. A. Remmerswaal, A. Kromm, G. Berden, S. van der Vorm, A. M. Rijs, H. S. Overkleeft, D. V. Filippov, F. P. J. T. Rutjes, G. A. van der Marel, J. Martens, J. Oomens, J. D. C. Codée, T. J. Boltje, *Nat. Commun.* **2020**, *11*, 2664.
[18] S. N. de Wildt, G. L. Kearns, J. S. Leeder, J. N. van den Anker, *Clin. Pharmacokinet.* **1999**, *36*, 439–452.
[19] a) J. Dinkelaar, A. R. de Jong, R. van Meer, M. Somers, G. Lodder, H. S. Overkleeft, J. D. C. Codée, G. A. van der Marel, *J. Org. Chem.* **2009**, *74*, 4982–4991; b) T. Hansen, S. van der Vorm, C. Tugny, W. A. Remmerswaal, J. M. A. van Hengst, G. A. van der Marel, J. D. C. Codée in *Comprehensive Glycoscience* (Ed.: J. Barchi Jr.), Elsevier, Oxford, **2021**, pp. 83–102; c) M. T. C. Walvoort, G. Lodder, J. Mazurek, H. S. Overkleeft, J. D. C. Codée, G. A. van der Marel, *J. Am. Chem. Soc.* **2009**, *131*, 12080–12081.
[20] L. Ayala, C. G. Lucero, J. A. C. Romero, S. A. Tabacco, K. A. Woerpel, *J. Am. Chem. Soc.* **2003**, *125*, 15521–15528.
[21] H. Xiao, G. Wang, P. Wang, Y. Li, *Chin. J. Chem.* **2010**, *28*, 1229–1232.
[22] J. Martens, G. Berden, C. R. Gebhardt, J. Oomens, *Rev. Sci. Instrum.* **2016**, *87*, 103108.
[23] J. Martens, J. Grzetic, G. Berden, J. Oomens, *Nat. Commun.* **2016**, *7*, 11754.
[24] L. Barnes, A.-R. Allouche, S. Chambert, B. Schindler, I. Compagnon, *Int. J. Mass Spectrom.* **2020**, *447*, 116235.
[25] T. Hansen, T. P. Ofman, J. G. C. Vlaming, I. A. Gagarinov, J. van Beek, T. A. Goté, J. M. Tichem, G. Ruijgrok, H. S. Overkleeft, D. V. Filippov, G. A. van der Marel, J. D. C. Codée, *Angew. Chem. Int. Ed.* **2021**, *60*, 937–945; *Angew. Chem.* **2021**, *133*, 950–958.
[26] a) J. M. Madern, T. Hansen, E. R. van Rijssel, H. A. V. Kistemaker, S. van der Vorm, H. S. Overkleeft, G. A. van der Marel, D. V. Filippov, J. D. C. Codée, *J. Org. Chem.* **2019**, *84*, 1218–1227; b) S. van der Vorm, T. Hansen, E. R. van Rijssel, R. Dekkers, J. M. Madern, H. S. Overkleeft, D. V. Filippov, G. A. van der Marel, J. D. C. Codée, *Chem. Eur. J.* **2019**, *25*, 7149–7157.
[27] C. G. Lucero, K. A. Woerpel, *J. Org. Chem.* **2006**, *71*, 2641–2647.
[28] a) J. S. Prell, T. M. Chang, J. A. Biles, G. Berden, J. Oomens, E. R. Williams, *J. Phys. Chem. A* **2011**, *115*, 2745–2751; b) F. A. M. G. van Geenen, R. F. Kranenburg, A. C. van Asten, J. Martens, J. Oomens, G. Berden, *Anal. Chem.* **2021**, *93*, 2687–2693; c) W. A. Remmerswaal, K. J. Houthuijs, R. van de Ven, H. Elferink, T. Hansen, G. Berden, H. S. Overkleeft, G. A. van der Marel, F. P. J. T. Rutjes, D. V. Filippov, T. J. Boltje, J. Martens, J. Oomens, J. D. C. Codée, *J. Org. Chem.* **2022**, *87*, 9139–9147.
[29] a) H. Liu, S.-Y. Zhou, G.-E. Wen, X.-X. Liu, D.-Y. Liu, Q.-J. Zhang, R. R. Schmidt, J.-S. Sun, *Org. Lett.* **2019**, *21*, 8049–8052; b) H. Liu, T. Hansen, S.-Y. Zhou, G.-E. Wen, X.-X. Liu, Q.-J. Zhang, J. D. C. Codée, R. R. Schmidt, J.-S. Sun, *Org. Lett.* **2019**, *21*, 8713–8717.

Manuscript received: June 5, 2022
Accepted manuscript online: August 12, 2022
Version of record online: September 12, 2022